AAC Journals.ASM.org

Post-PKS Tailoring Steps of the Spiramycin Macrolactone Ring in *Streptomyces ambofaciens*

Hoang-Chuong Nguyen,[a,b,c] Emmanuelle Darbon,[a,b] Robert Thai,[d] Jean-Luc Pernodet,[a,b] Sylvie Lautru[a,b]

Université Paris-Sud, Institut de Génétique et Microbiologie (UMR 8621), Orsay, France[a]; CNRS, Institut de Génétique et Microbiologie (UMR 8621), Orsay, France[b]; University of Science, Viet Nam National University in Ho Chi Minh City, Ho Chi Minh City, Vietnam[c]; CEA, iBiTecS, Service d'Ingénierie Moléculaire des Protéines, Gif-sur-Yvette, France[d]

Spiramycins are clinically important 16-member macrolide antibiotics produced by *Streptomyces ambofaciens*. Biosynthetic studies have established that the earliest lactonic intermediate in spiramycin biosynthesis, the macrolactone platenolide I, is synthesized by a type I modular polyketide synthase (PKS). Platenolide I then undergoes a series of post-PKS tailoring reactions yielding the final products, spiramycins I, II, and III. We recently characterized the post-PKS glycosylation steps of spiramycin biosynthesis in *S. ambofaciens*. We showed that three glycosyltransferases, Srm5, Srm29, and Srm38, catalyze the successive attachment of the three carbohydrates mycaminose, forosamine, and mycarose, respectively, with the help of two auxiliary proteins, Srm6 and Srm28. However, the enzymes responsible for the other tailoring steps, namely, the C-19 methyl group oxidation, the C-9 keto group reduction, and the C-3 hydroxyl group acylation, as well as the timing of the post-PKS tailoring reactions, remained to be established. In this study, we show that Srm13, a cytochrome P450, catalyzes the oxidation of the C-19 methyl group into a formyl group and that Srm26 catalyzes the reduction of the C-9 keto group, and we propose a timeline for spiramycin-biosynthetic post-PKS tailoring reactions.

Spiramycins are macrolide antibiotics produced by *Streptomyces ambofaciens* and used in human medicine for their activities against bacteria and *Toxoplasma* spp. (1–4). They are composed of a 16-member lactone ring, on which three sugars (mycaminose, forosamine, and mycarose) are attached (Fig. 1). Spiramycin biosynthesis has been studied for more than 30 years, and numerous studies have contributed to the isolation of the spiramycin-biosynthetic *srm* genes (Fig. 1) (5–8) and the characterization of biosynthetic steps (9, 10). These studies established that the macrolactone ring, called platenolide I (compound 1), is synthesized through the repeated condensation of carboxylic acid units catalyzed by a type I modular polyketide synthase (PKS) (7). In this PKS, module 3 (Srm9) is responsible for the incorporation of the C-9–C-10 unit and module 4 (the first module of Srm10) contains a ketoreductase (KR) domain that could catalyze the reduction of the C-9 keto group. However, this domain has been suggested to be inactive (7). This is consistent with the oxidation state of C-9 (keto group) in platenolide I.

Several post-PKS tailoring steps are required to ensure the synthesis of the final molecules, spiramycins I, II, and III. These include oxidation of the C-19 methyl group, reduction of the C-9 keto group, attachment of the mycaminose, forosamine, and mycarose sugars, and acylation of the C-3 hydroxyl group. Some of the genes required for these tailoring steps have been identified. Thus, the genes required for the biosynthesis of the three sugars from the common precursor glucose-1-phosphate are encoded within the *srm* gene cluster (8), and we recently characterized the glycosylation steps in *S. ambofaciens* (10). We showed that three glycosyltransferases, Srm5, Srm29, and Srm38, successively catalyze the attachment of mycaminose, forosamine, and mycarose, respectively, with the help of two auxiliary proteins, Srm6 and Srm28. However, the *srm* genes responsible for the other post-PKS tailoring steps remain to be identified.

The first glycosylated intermediate in spiramycin biosynthesis, observed in the culture supernatant of a *srm29* deletion mutant, is forocidin (compound 4) (Fig. 1). In this molecule, platenolide I has already undergone two modifications, in addition to the attachment of the mycaminose: the reduction of the C-9 keto group and the oxidation of the C-19 methyl group. Although it is clear that the reduction of C-9 keto group occurs prior to the attachment of the second sugar, forosamine, this observation also suggests that the oxidation of the C-19 methyl group precedes the glycosylation of forocidin by Srm29. In this study, we undertook the identification of the genes involved in the reduction of the C-9 keto group and the oxidation of the C-19 methyl group of platenolide I, and we attempted to establish a timeline for the various tailoring steps. We showed that Srm13 catalyzes the oxidation of the C-19 methyl group, as proposed previously (8). We demonstrated that among the three potential candidate genes (*srm26*, *srm42*, and *srm43*), *srm26* encodes the post-PKS ketoreductase involved in the reduction of the C-9 keto group. Furthermore, analysis of the biosynthetic intermediates strongly suggests that the reduction of the C-9 keto group of platenolide I occurs first and that the glycosylation of the lactone ring by Srm5 precedes the oxidation of the C-19 methyl group.

Received 13 March 2013 Returned for modification 25 March 2013
Accepted 23 May 2013
Published ahead of print 28 May 2013
Address correspondence to Sylvie Lautru, sylvie.lautru@igmors.u-psud.fr.
H.-C.N. and E.D. contributed equally to this article.
Supplemental material for this article may be found at http://dx.doi.org/10.1128/AAC.00512-13.

doi:10.1128/AAC.00512-13

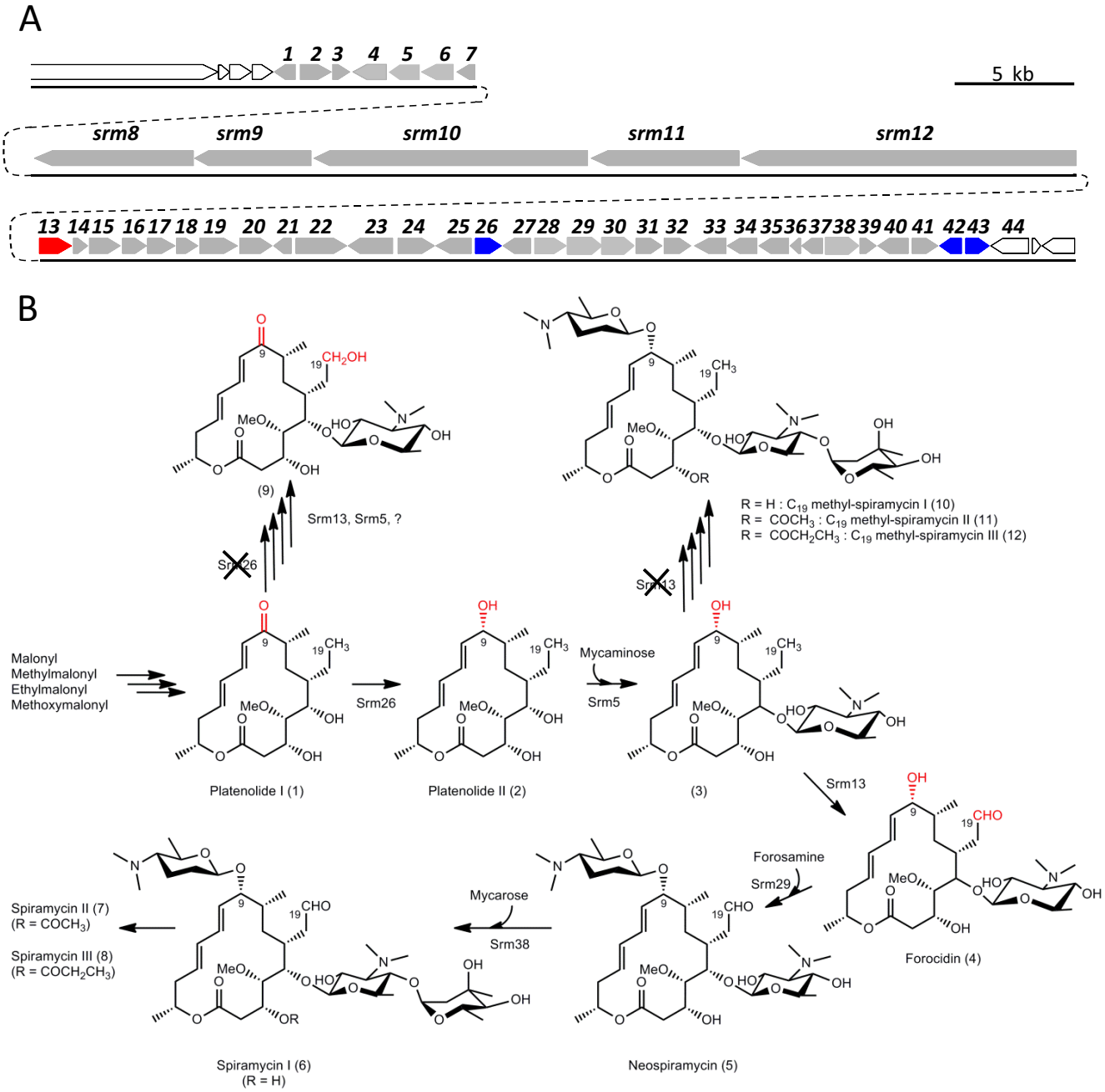

FIG 1 Spiramycin biosynthesis. (A) Spiramycin biosynthetic cluster with the three putative reductase genes *srm26*, *srm42*, and *srm43* represented by blue arrows and *srm13* represented by a red arrow. (B) Proposed biosynthetic pathway for the post-PKS tailoring steps.

MATERIALS AND METHODS

Strains, plasmids, and culture conditions. The strains and plasmids used in this study are listed in Table S1 in the supplemental material. *Escherichia coli* and *S. ambofaciens* strains were grown in standard media with appropriate antibiotics as necessary (11, 12). For spiramycin production, *S. ambofaciens* strains were grown in MP5 medium (13).

Preparation and manipulation of DNA. DNA extraction and manipulation, *E. coli* transformation, and *E. coli-Streptomyces* conjugation were performed according to standard procedures (11, 12). DNA amplifications were carried out using either *Taq* polymerase from Qiagen, the GC-rich PCR system from Roche, or Phusion DNA polymerase from Thermo Fisher Scientific.

Inactivation of *srm13*, *srm26*, *srm42*, and *srm43*. Each of the genes *srm13*, *srm26*, *srm42*, and *srm43* was individually inactivated by gene replacement in *S. ambofaciens* strain OSC2, resulting in the deletion of most of the coding sequence of each gene and its replacement by a cassette containing an apramycin resistance gene.

The same strategy was used for inactivating *srm13*, *srm26*, and *srm42*. For *srm13*, two DNA fragments flanking the gene were PCR amplified: a 2.2-kb upstream fragment (amplified with primers SRM13 and SRM14 [see Table S2 in the supplemental material]), overlapping the beginning of the *srm13* coding sequence and carrying HindIII and EcoRV restriction sites at the ends of the fragment, and a 2-kb downstream fragment (amplified with primers SRM15 and SRM16), overlapping the end of the

srm13 coding sequence and carrying EcoRV and NheI restriction sites at the ends of the fragment. The excisable cassette *att3aac*, conferring resistance to apramycin, was recovered by digestion of plasmid pOSV234 by EcoRV. Then the upstream and downstream fragments of *srm13* were cloned into cosmid pWED2 cut by HindIII and NheI, in the same relative orientation as in the *S. ambofaciens* chromosome, on each side of the *att3aac* cassette, resulting in cosmid pSPM573. pSPM573 was introduced into *S. ambofaciens* OSC2 by *E. coli-Streptomyces* conjugation using *E. coli* ET12567/pUZ8002, and apramycin selection was applied. Apramycin-resistant *S. ambofaciens* clones were screened for sensitivity to puromycin, indicating a double-crossover allelic exchange. This was confirmed by PCR (data not shown). The resulting *S. ambofaciens* Δ*srm13*::*att3aac* mutant strain was called SPM512. The apramycin resistance cassette inserted into *srm13* of strain SPM512 was then excised by site-specific recombination using plasmid pOSV236 containing genes encoding the excisionase and the integrase from pSAM2 (10). pOSV236 was introduced into SPM512 by conjugation with *E. coli* ET12567/pUZ8002/pOSV236. Apramycin-sensitive, thiostrepton-resistant clones were screened. Plasmid pOSV236 was lost after a few rounds of growth without antibiotic selection. The excision of the cassette leaving a scar of 33 bp (*att3*) was confirmed by PCR and sequencing (data not shown). The resulting strain with an in-frame deletion of *srm13* (Δ*srm13*::*att3*) was called SPM513. A similar strategy using the excisable cassette *att2aac* was employed to construct the *srm26* in-frame mutant strain (SPM235) and the *srm42* mutant strain (SPM225). For the *srm42* mutant strain, the *att2aac* cassette was not excised.

PCR-targeting technology was used for the inactivation of *srm43* (14). Cosmid pSPM36, a pWED2 derivative containing part of the spiramycin-biosynthetic gene cluster, including *srm43*, was introduced into *E. coli* strain KS272 containing pKOBEG and expressing the phage λ red functions (15). The resulting strain was transformed with a PCR product obtained with primer pair EDR71/EDR72 and consisting of the excisable cassette *att3aac* flanked by 40-bp sequences identical to those at the beginning and end of the *srm43* coding region. After λ red-mediated recombination, the resulting cosmid, pSPM543, was introduced into *S. ambofaciens* OSC2 by interspecific transfer from *E. coli* S17-1, and apramycin selection was applied. Apramycin-resistant *S. ambofaciens* clones were screened for sensitivity to puromycin, indicating a double-crossover allelic exchange. This was confirmed by PCR (data not shown). The resulting *S. ambofaciens* Δ*srm43*::*att3aac* mutant strain was called SPM543.

Construction of the Δ*srm13* Δ*srm26* double mutant. The Δ*srm13* Δ*srm26* double mutant was produced by introduction of the pSPM573 plasmid into *S. ambofaciens* SPM235 by interspecific transfer from *E. coli* ET12597/pUZ8002/pSPM573. Apramycin-resistant *S. ambofaciens* clones were screened for sensitivity to puromycin, indicating a double-crossover allelic exchange. This was confirmed by PCR (data not shown). The resulting *S. ambofaciens* Δ*srm13*::*att3aac* Δ*srm26*::*att2* mutant strain was called SPM514. The apramycin resistance cassette was then excised by site-specific recombination using plasmid pOSV236. The excision of the cassette leaving a scar of 33 bp (*att3*) was confirmed by PCR and sequencing (data not shown). The resulting mutant strain (Δ*srm13*::*att3* Δ*srm26*::*att2*) was called SPM515.

Construction of plasmid pSPM266 expressing *srm26*. A fragment of 1.4 kb containing the complete *srm26* coding region, with upstream and downstream sequences, was obtained by PCR amplification with oligonucleotides OE.srm26F and OE.srm26R as primers and with *S. ambofaciens* total genomic DNA as the template. The product was cloned as a HindIII-EcoRI fragment into vector pOSV206 digested with the same enzymes, yielding plasmid pSPM266. In this multicopy vector, *srm26* is expressed under the control of the strong and constitutive promoter *ermE*p*.

LC-MS analysis. After 4 days of culture at 27°C, supernatants were filtered through Ultrafree-MC filters (0.1 μm; Millipore) and were analyzed on an Atlantis dC_{18} column (length, 250 mm; inner diameter, 4.6 mm; particle size, 5 μm; column temperature, 25°C) using an Agilent 1100 high-performance liquid chromatography (HPLC) instrument equipped with a binary pump. Samples were eluted with isocratic 0.1% HCOOH in H_2O (solvent A)–0.1% HCOOH in CH_3CN (solvent B) (95:5) at 1 ml min^{-1} for 5 min, followed by a gradient to 50:50 (solvent A to solvent B) over 35 min. A Bruker Daltonik Esquire HCT ion trap mass spectrometer (MS) equipped with an orthogonal atmospheric pressure interface-electrospray ionization (AP-ESI) source was coupled online to the HPLC system and was used for MS and tandem MS (MS-MS) analyses. Elution from the Atlantis dC_{18} column was split into two flows: 1/10 was directed to an ESI mass spectrometer for MS and MS-MS measurements and the remaining 9/10 to a diode array UV detector. In the ESI process, nitrogen served as the drying and nebulizing gas, and helium gas was introduced into the ion trap both for efficient trapping and cooling of the ions generated by ESI and for fragmentation processes. Ionization was carried out in positive mode with a nebulizing gas set at 241 kPa, a drying gas set at 8 μl/min, and a drying temperature set at 345°C for optimal spray and desolvation. Ionization and mass analysis conditions (capillary high voltage, skimmer and capillary exit voltages, and ion transfer parameters) were tuned for optimal detection of compounds in the range of masses between 100 and 1,000 *m/z*.

Bioassays. The antibacterial activity of spiramycin or spiramycin derivatives (C-19-methyl-spiramycins) was analyzed as described previously (16). Briefly, culture supernatants of *S. ambofaciens* and defined quantities of spiramycins were applied to Whatman Aa paper disks that were laid on plates containing *Micrococcus luteus. The M. luteus* strain used was resistant to congocidine, an antibiotic also produced by *S. ambofaciens*, together with spiramycin, in MP5 medium.

RESULTS AND DISCUSSION

Srm13 catalyzes the oxidation of the lactone ring C-19 methyl group into a formaldehyde moiety. In a previous study, we proposed that Srm13, which encodes a cytochrome P450, could catalyze the oxidation of the C-19 methyl group of the lactone ring into a formaldehyde moiety during spiramycin biosynthesis (8). Indeed, Srm13 presents some sequence similarities with other cytochromes P450 known to be involved in the oxidation of the methyl group equivalent to the C-19 methyl group of spiramycin in other 16-member ring macrolide antibiotics (67% identity and 79% similarity with TylI, involved in tylosin biosynthesis; 63% identity and 77% similarity with RosC, involved in rosamicin biosynthesis) (17, 18) (see Fig. S1 in the supplemental material for the tylosin and rosamicin structures and the positions modified by TylI and RosC).

To verify our hypothesis, we constructed a *srm13* in-frame deletion mutant in OSC2, designated SPM513. After 4 days of culture of SPM513 in MP5 medium, the supernatant was analyzed by LC-MS. Comparison of the UV chromatogram (232 nm) of SPM513 with the UV chromatogram of the wild-type strain OSC2 (Fig. 2A) and analysis of the extracted ion current (EIC) chromatograms at *m/z* values corresponding to those of the three spiramycins (Fig. 2B, peaks 6, 7, and 8) indicated that the production of spiramycins was abolished in SPM513 (data not shown). However, the mutant accumulated three new metabolites (peaks 10, 11, and 12 [Fig. 2C and D]) that differ from spiramycins I, II, and III by 16 mass units, consistent with the lack of an oxygen residue. These compounds were identified as C-19-methyl-spiramycins I, II, and III (compounds 10, 11, and 12 [Fig. 1]) by their masses and fragmentation patterns (compared with the fragmentation patterns of spiramycins I, II, and III [19, 20]) (see also Fig. S2 in the supplemental material). This result clearly demonstrates that Srm13 catalyzes the conversion of the C-19 methyl group of the spiramycin lactone ring into a formaldehyde moiety. It also suggests that either this oxidation is the final step in spiramycin bio-

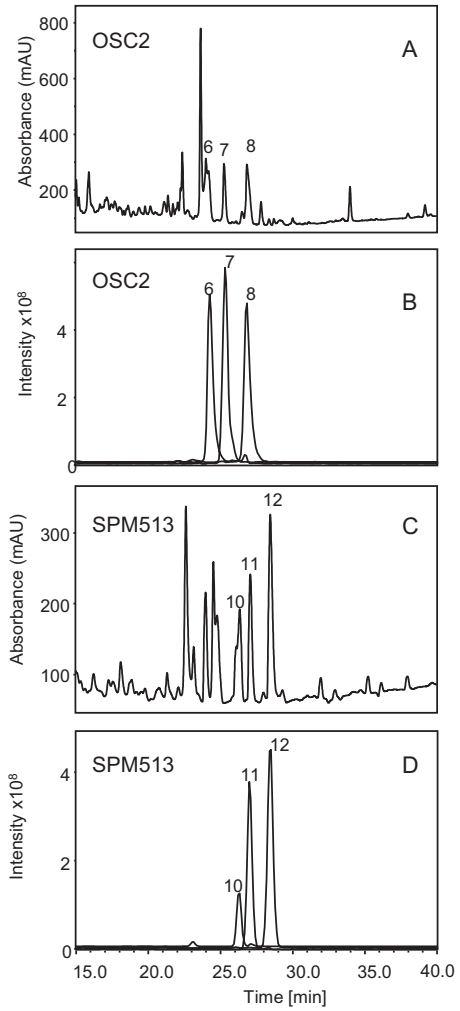

FIG 2 LC and LC-MS analyses of culture supernatants of the wild-type strain (OSC2) and the Δ*srm13* deletion mutant (SPM513). (A and B) UV (A) and EIC (B) traces of *m/z* 422.2 ($[M + 2H]^{2+}$) (peak 6), *m/z* 443.2 ($[M + 2H]^{2+}$) (peak 7), and *m/z* 450.2 ($[M + 2H]^{2+}$) (peak 8) for OSC2. (C and D) UV (C) and EIC (D) traces of *m/z* 415.2 ($[M + 2H]^{2+}$) (peak 10), *m/z* 436.2 ($[M + 2H]^{2+}$) (peak 11), and *m/z* 443.2 ($[M + 2H]^{2+}$) (peak 12) for SPM513. Peak numbers refer to molecule numbers in Fig. 1.

synthesis or, if it occurs earlier in spiramycin biosynthesis, the absence of Srm13 does not prevent downstream tailoring reactions.

Rosamicin is a macrolide antibiotic structurally related to spiramycin. The rosamicin derivative devoid of the C-20 formyl group (RS-B) (equivalent to the spiramycin C-19 methyl group) is 10 to 60 times less active than rosamicin, suggesting that this group is important to the antibacterial activity of rosamicin (18). To determine whether the C-19-methyl-spiramycin derivatives possess some antibacterial activity, culture supernatants of strain SPM513 were tested by a bioassay. No growth inhibition was observed around the disks soaked in SPM513 culture supernatants, yet a rough estimation of the production of the C-19-methyl-spiramycin derivatives (based on LC and EIC chromatograms) suggests that this production is comparable to spiramycin production in the wild-type strain OSC2 (50 to 100 μg/ml). In the bioassay, we can routinely detect spiramycin concentrations as low as 1 μg/ml. Thus, this finding indicates that C-19-methyl-spiramycins are much less active than spiramycins and that, as with rosamicin, the C-19 formyl moiety of spiramycin is essential to antibacterial activity.

Three *srm* genes are potential candidates for the reduction of the C-9 keto group. Platenolide I, a known spiramycin biosynthetic intermediate (21), bears a keto group at the C-9 position. This keto group has to be reduced into a hydroxyl group prior to the attachment of the forosamine sugar. Post-PKS reduction of polyketide keto groups has been described previously, for example, in the biosynthesis of avermectin, in which AveF catalyzes the reduction of the avermectin aglycon C-5 keto group (22). Other examples include MilF, a homologue of AveF in milbemycin biosynthesis (23), and MtmW, catalyzing the reduction of the C-4′ keto group in mithramycin biosynthesis (24). However, bioinformatic analysis failed to detect any homologues of these post-PKS ketoreductases in the *srm* gene cluster.

Analysis of the *srm* gene cluster previously led us to propose Srm43, a 324-amino-acid protein predicted by CD-Search (25) to belong to the aldo-keto reductase superfamily of NAD(P)H oxidoreductases, as a potential candidate for the catalysis of the C-9 keto group reduction (8). However, two other Srm proteins of the four with no assigned function in spiramycin biosynthesis could fulfill this function: Srm42 and Srm26. Srm42 is a 285-amino-acid protein presenting some similarities to triphenylmethane reductase (TMR)-like proteins and proteins of the atypical short-chain dehydrogenase/reductase (SDR) family. Srm26 is a protein of 347 amino acid residues potentially belonging to the atypical SDR family of proteins. Both Srm42 and Srm26 possess a predicted NAD(P)H binding site. We therefore decided to inactivate each of these three genes, *srm26*, *srm42*, and *srm43*, to determine which of them codes for the post-PKS ketoreductase responsible for the C-9 keto reduction of platenolide I.

Srm42 and Srm43 are not involved in spiramycin biosynthesis. To evaluate the potential involvement of *srm42* and *srm43* in the reduction of the platenolide C-9 keto group, the two genes were replaced by an apramycin resistance cassette (*att2aac*) in the wild-type strain OSC2, yielding strains SPM225 and SPM543, respectively. Analysis of the culture supernatants of these mutant strains by LC-MS showed that spiramycins I, II, and III are still produced (see Fig. S3 in the supplemental material), indicating that *srm42* and *srm43* are not involved in the reduction of the platenolide I C-9 keto group or in spiramycin biosynthesis. Thus, the *srm* gene cluster, previously delimited at *srm43* (26), most likely ends with *srm41*.

Srm26 catalyzes platenolide C-9 ketoreduction. The *srm26* gene was replaced by the apramycin resistance cassette (*att2aac*) in the wild-type OSC2 strain, yielding SPM234. The cassette was then excised using the unstable pOSV236 plasmid expressing the pSAM2 excisionase and integrase (10), yielding mutant strain SPM235. LC-MS analysis of the SPM235 culture supernatant showed that production of spiramycins was abolished (data not shown), demonstrating that *srm26* is involved in spiramycin biosynthesis. To determine whether Srm26 catalyzes the reduction of the keto group at the C-9 position of platenolide I, we used LC-MS data to search for the presence of known or potential spiramycin biosynthetic intermediates, including platenolides I (compound 1) and II (compound 2). Figure 3A shows that SPM235 accumulates platenolide I (peak 1) but not platenolide II (Fig. 3B, peak 2). However, the figure also shows that SPM235 accumulates a small

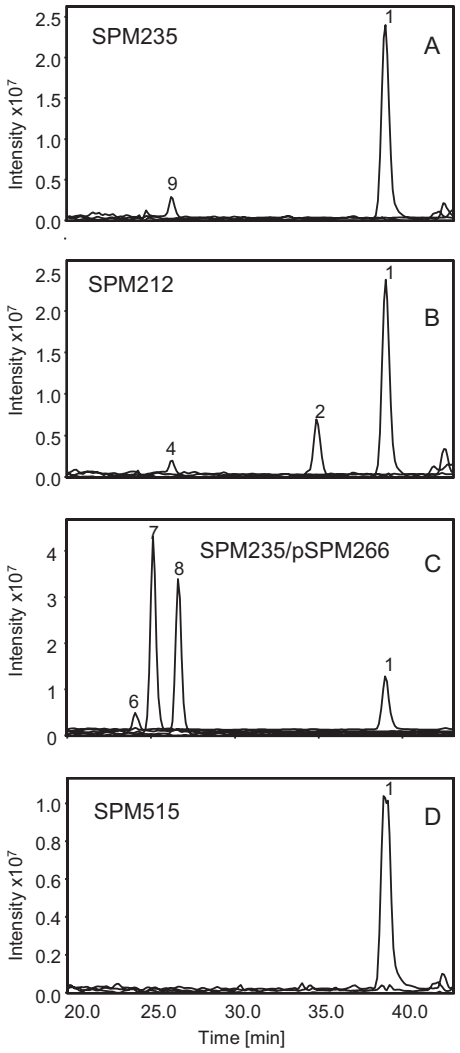

FIG 3 Identification of the gene catalyzing the reduction of the C-9 keto group of platenolide I by LC-MS analyses. (A) EIC traces for *m/z* 556.3 ($[M + H]^+$) (peak 9) and *m/z* 391.0 ($[M + Na]^+$) (peak 1) for the *srm26* deletion mutant (SPM235). (B) EIC traces of *m/z* 556.3 ($[M + H]^+$) (peak 4), *m/z* 391.0 ($[M + Na]^+$) (peak 1), and *m/z* 393.0 ($[M + Na]^+$) (peak 2) for strain SPM212 (*srm28* deletion mutant) accumulating forocidin (peak 4). (C) EIC traces of *m/z* 422.2 ($[M + 2H]^{2+}$) (peak 6), *m/z* 443.2 ($[M + 2H]^{2+}$) (peak 7), and *m/z* 450.2 ($[M + 2H]^{2+}$) (peak 8) for genetically complemented SPM235. (D) EIC traces of *m/z* 391.0 ($[M + Na]^+$) (peak 1) for the *srm26 srm13* double deletion mutant (SPM515). Peak numbers refer to molecule numbers in Fig. 1.

amount of a compound (Fig. 3A, peak 9) with the same mass and retention time as forocidin (compound 4) (Fig. 3B, peak 4). This was unexpected, because forocidin, a known spiramycin biosynthetic intermediate, is hydroxylated at the C-9 position. Thus, if Srm26 catalyzes the reduction of the keto group on C-9, a *srm26* deletion mutant should not accumulate forocidin. Moreover, were forocidin to be produced, downstream biosynthetic steps should occur and spiramycins should be produced. To rule out the possibility of a mutation elsewhere in the *srm* gene cluster, we genetically complemented the *srm26* deletion mutant. We cloned *srm26* into the replicative vector pOSV206 and introduced the resulting plasmid, pSPM266, into SPM235. LC-MS analysis of the culture supernatant of SPM235/pSPM266 shows that production of spiramycins I, II, and III is restored (Fig. 3C), indicating that the observed chemotype for strain SPM235 is due solely to the deletion of *srm26*.

Another form of spiramycin, spiramycin IV (see Fig. S4 in the supplemental material), has been described elsewhere (9). Spiramycin IV is a C-19-hydroxylated (reduced) form of spiramycin I. We hypothesized that compound 9 may correspond to the C-19-hydroxylated, C-9-oxidized form of forocidin, an isomer of forocidin that could elute at the same retention time. To verify our hypothesis, we constructed a *srm13 srm26* double deletion mutant (SPM515). LC-MS analysis of the SPM515 culture supernatant reveals only the presence of platenolide I (compound 1) (Fig. 3D, peak 1), supporting the hypothesis that compound 9 is the C-19-hydroxylated, C-9-oxidized form of forocidin. The presence of a hydroxyl group on C-19 may suggest that oxidation of the C-19 methyl group into a formyl group by Srm13 goes through a hydroxyl intermediate, as has been proposed for rosamicin biosynthesis (18). However, the C-19 formyl, C-9 keto form of forocidin was not detected in the SPM515 culture supernatant, as would be expected in this case. Thus, the C-19 hydroxyl, C-9 keto form of forocidin may result from a nonspecific reduction of the C-19 formyl group of the C-9-oxidized form of forocidin, as observed for the conversion of tylosin to relomycin (27). Taken together, these experiments demonstrate that Srm26 is the post-PKS reductase catalyzing the reduction of the platenolide I C-9 keto group, yielding platenolide II.

Proposed model for the timing of the post-PKS platenolide tailoring reactions. Previous studies (10) have established that glycosylation of the spiramycin aglycon occurs in the following order: addition of mycaminose catalyzed by Srm5 (yielding forocidin [compound 4]), followed by addition of forosamine by Srm29 (yielding neospiramycin I [compound 5]), and finally addition of mycarose by Srm38 (yielding spiramycin I [compound 6]). Although it is clear that the reduction of the C-9 keto group of the platenolide has to occur prior to the attachment of the second sugar, forosamine, the timing of this reduction, of the first glycosylation, and of the C-19 methyl oxidation is not clear. To try to determine whether these reactions occur in a strict or partially defined order, we used LC-MS to analyze our mutant strains in which post-PKS tailoring steps were affected, looking for intermediates that could potentially accumulate depending on the timing of these tailoring steps. The *srm26* deletion mutant SPM235 did not accumulate the C-19 formyl form of platenolide I, suggesting that the oxidation of the C-19 methyl group occurs after the reduction of the C-9 keto group. The *srm5* deletion mutant SPM121 accumulates platenolide I and platenolide II, but not the C-19 formyl forms of these molecules (10) (data not shown), suggesting that the addition of the first sugar, mycaminose, occurs prior to the oxidation of the C-19 methyl group. The *srm13* deletion mutant SPM513 accumulates the C-19 methyl forms of spiramycin, indicating that the absence of Srm13 does not prevent downstream tailoring reactions, but not pointing to the specific timing of the C-19 methyl oxidation. However, the *srm29* deletion mutant SPM108 accumulates only one form of glycosylated platenolide, forocidin (compound 4), in which C-9 is reduced (hydroxyl group) and C-19 is oxidized (formyl group), suggesting that the oxidation of the C-19 methyl group occurs prior to the addition of the second sugar, forosamine.

Thus, based on these data, we propose that after platenolide I is released from the spiramycin-biosynthetic enzyme PKS, the re-

duction of the C-9 keto group occurs first (yielding platenolide II), followed successively by glycosylation by Srm5 (yielding compound 3), the oxidation of the C-19 methyl group (yielding forocidin), the addition of forosamine by Srm29 (yielding neospiramycin), and, finally, the addition of mycarose by Srm38, yielding spiramycin I (Fig. 1B). The acylation of spiramycin I to yield spiramycins II and III may be catalyzed by Srm2 (8). The timing of the post-PKS tailoring reactions proposed here is similar to what has been observed in the biosyntheses of two other 16-member macrolides, tylosin and rosamicin, biosyntheses in which the glycosylation of the C-5 hydroxyl group occurs prior to the oxidation of the C-20 methyl group (18, 28). Moreover, in *Streptomyces fradiae*, the absence of TylI, the homologue of Srm13 involved in tylosin biosynthesis, is likely to result in the synthesis of C-20-methyl tylosin, an outcome similar to that observed for the *srm13* deletion mutant, which produces C-19-methyl-spiramycins. However, to our knowledge, in the literature, only a mutant in which both *tylI* and *tylD* (a gene involved in the biosynthesis of 6-deoxy-D-allose, the third sugar to be attached to the lactone ring) are affected has been described (29). In that strain, all post-PKS tailoring steps possible in the absence of 6-deoxy-D-allose occur.

In conclusion, we have identified in this study the enzymes involved in two important platenolide I tailoring steps. We showed that Srm13 catalyzes the oxidation of the C-19 methyl group into a formyl group, a group that appears, as for rosamicin, to be important for the biological activity of spiramycins. We also demonstrated that Srm26 catalyzes the reduction of the C-9 keto group into a hydroxyl group, allowing downstream glycosylation at this position. It has been demonstrated that *S. ambofaciens* fed with tylactone, the first lactonic intermediate of tylosin, is able to convert it into spiramycin-tylosin hybrids, the chimeramycins (30). This suggests a relative flexibility of Srm26 with regard to its macrolactone substrate and opens the way to the biosynthesis of new hybrid 16-member macrolide antibiotics.

ACKNOWLEDGMENTS

H.-C.N. received fellowships from the Vietnamese Ministry of Education and from the Université Paris-Sud. This work was supported in part by the European Union through the Integrated Project ActinoGEN (CT-2004-0005224) and by the Pôle de Recherche et d'Enseignement Supérieur UniverSud Paris.

We thank Maud Juguet for the construction of the pOSV206 vector and Adeline Valadié for technical assistance.

REFERENCES

1. **Chew WK, Segarra I, Ambu S, Mak JW.** 2012. Significant reduction of brain cysts caused by *Toxoplasma gondii* after treatment with spiramycin coadministered with metronidazole in a mouse model of chronic toxoplasmosis. Antimicrob. Agents Chemother. **56:**1762–1768.
2. **Valentini P, Annunziata ML, Angelone DF, Masini L, De Santis M, Testa A, Grillo RL, Speziale D, Ranno O.** 2009. Role of spiramycin/cotrimoxazole association in the mother-to-child transmission of toxoplasmosis infection in pregnancy. Eur. J. Clin. Microbiol. Infect. Dis. **28:**297–300.
3. **Poulet P-P, Duffaut D, Barthet P, Brumpt I.** 2005. Concentrations and *in vivo* antibacterial activity of spiramycin and metronidazole in patients with periodontitis treated with high-dose metronidazole and the spiramycin/metronidazole combination. J. Antimicrob. Chemother. **55:**347–351.
4. **Dumitrescu AL (ed).** 2011. Antibiotics and antiseptics in periodontal therapy. Springer, Berlin, Germany.
5. **Richardson MA, Kuhstoss S, Huber ML, Ford L, Godfrey O, Turner JR, Rao RN.** 1990. Cloning of spiramycin biosynthetic genes and their use in constructing *Streptomyces ambofaciens* mutants defective in spiramycin biosynthesis. J. Bacteriol. **172:**3790–3798.
6. **Geistlich M, Losick R, Turner JR, Rao RN.** 1992. Characterization of a novel regulatory gene governing the expression of a polyketide synthase gene in *Streptomyces ambofaciens*. Mol. Microbiol. **6:**2019–2029.
7. **Kuhstoss S, Huber M, Turner JR, Paschal JW, Rao RN.** 1996. Production of a novel polyketide through the construction of a hybrid polyketide synthase. Gene **183:**231–236.
8. **Karray F, Darbon E, Oestreicher N, Dominguez H, Tuphile K, Gagnat J, Blondelet-Rouault MH, Gerbaud C, Pernodet J-L.** 2007. Organization of the biosynthetic gene cluster for the macrolide antibiotic spiramycin in *Streptomyces ambofaciens*. Microbiology (Reading, Engl.) **153:**4111–4122.
9. **Ōmura S (ed).** 1984. Macrolide antibiotics: chemistry, biology, and practice. Academic Press, Orlando, FL.
10. **Nguyen HC, Karray F, Lautru S, Gagnat J, Lebrihi A, Huynh TDH, Pernodet J-L.** 2010. Glycosylation steps during spiramycin biosynthesis in *Streptomyces ambofaciens*: involvement of three glycosyltransferases and their interplay with two auxiliary proteins. Antimicrob. Agents Chemother. **54:**2830–2839.
11. **Sambrook J, Russell DW.** 2001. Molecular cloning: a laboratory manual, 3rd ed. Cold Spring Harbor Laboratory Press, Cold Spring Harbor, NY.
12. **Kieser T, Bibb MJ, Buttner MJ, Chater KK, Hopwood DA.** 2000. Practical *Streptomyces* genetics. John Innes Foundation, Norwich, United Kingdom.
13. **Pernodet JL, Alegre MT, Blondelet-Rouault MH, Guérineau M.** 1993. Resistance to spiramycin in *Streptomyces ambofaciens*, the producer organism, involves at least two different mechanisms. J. Gen. Microbiol. **139:**1003–1011.
14. **Gust B, Chandra G, Jakimowicz D, Yuqing T, Bruton CJ, Chater KF.** 2004. Lambda red-mediated genetic manipulation of antibiotic-producing *Streptomyces*. Adv. Appl. Microbiol. **54:**107–128.
15. **Chaveroche MK, Ghigo JM, D'Enfert C.** 2000. A rapid method for efficient gene replacement in the filamentous fungus *Aspergillus nidulans*. Nucleic Acids Res. **28:**e97. doi:10.1093/nar/28.22.e97.
16. **Gourmelen A, Blondelet-Rouault MH, Pernodet JL.** 1998. Characterization of a glycosyl transferase inactivating macrolides, encoded by *gimA* from *Streptomyces ambofaciens*. Antimicrob. Agents Chemother. **42:**2612–2619.
17. **Merson-Davies LA, Cundliffe E.** 1994. Analysis of five tylosin biosynthetic genes from the *tyllBA* region of the *Streptomyces fradiae* genome. Mol. Microbiol. **13:**349–355.
18. **Iizaka Y, Higashi N, Ishida M, Oiwa R, Ichikawa Y, Takeda M, Anzai Y, Kato F.** 2013. Function of cytochrome P450 enzymes RosC and RosD in the biosynthesis of rosamicin macrolide antibiotic produced by *Micromonospora rosaria*. Antimicrob. Agents Chemother. **57:**1529–1531.
19. **Pendela M, Govaerts C, Diana J, Hoogmartens J, Van Schepdael A, Adams E.** 2007. Characterization of impurities in spiramycin by liquid chromatography/ion trap mass spectrometry. Rapid Commun. Mass Spectrom. **21:**599–613.
20. **Van Poucke C, De Keyser K, Baltusnikiene A, McEvoy JD, Van Peteghem C.** 2003. Liquid chromatographic–tandem mass spectrometric detection of banned antibacterial growth promoters in animal feed. Anal. Chim. Acta **483:**99–109.
21. **Ōmura S, Kitao C, Hamada H, Ikeda H,.** 1979. Bioconversion and biosynthesis of 16-membered macrolide antibiotics. X. Final steps in the biosynthesis of spiramycin, using enzyme inhibitor: cerulenin. Chem. Pharm. Bull. (Tokyo) **27:**176–182.
22. **Ikeda H, Nonomiya T, Usami M, Ohta T, Omura S.** 1999. Organization of the biosynthetic gene cluster for the polyketide anthelmintic macrolide avermectin in *Streptomyces avermitilis*. Proc. Natl. Acad. Sci. U. S. A. **96:**9509–9514.
23. **Wang X-J, Wang C-Q, Sun X-L, Xiang W-S.** 2010. 5-Ketoreductase from *Streptomyces bingchengensis*: overexpression and preliminary characterization. Biotechnol. Lett. **32:**1497–1502.
24. **Remsing LL, González AM, Nur-e-Alam M, Fernández-Lozano MJ, Braña AF, Rix U, Oliveira MA, Méndez C, Salas JA, Rohr J.** 2003.

Mithramycin SK, a novel antitumor drug with improved therapeutic index, mithramycin SA, and demycarosyl-mithramycin SK: three new products generated in the mithramycin producer *Streptomyces argillaceus* through combinatorial biosynthesis. J. Am. Chem. Soc. **125:**5745–5753.
25. **Marchler-Bauer A, Bryant SH.** 2004. CD-Search: protein domain annotations on the fly. Nucleic Acids Res. **32:**W327–W331.
26. **Karray F, Darbon E, Nguyen HC, Gagnat J, Pernodet J-L.** 2010. Regulation of the biosynthesis of the macrolide antibiotic spiramycin in *Streptomyces ambofaciens*. J. Bacteriol. **192:**5813–5821.
27. **Huang SL, Hassell TC, Yeh WK.** 1993. Purification and properties of NADPH-dependent tylosin reductase from *Streptomyces fradiae*. J. Biol. Chem. **268:**18987–18993.
28. **Baltz RH, Seno ET, Stonesifer J, Wild GM.** 1983. Biosynthesis of the macrolide antibiotic tylosin. A preferred pathway from tylactone to tylosin. J. Antibiot. **36:**131–141.
29. **Baltz RH, Seno ET.** 1981. Properties of *Streptomyces fradiae* mutants blocked in biosynthesis of the macrolide antibiotic tylosin. Antimicrob. Agents Chemother. **20:**214–225.
30. **Ōmura S, Sadakane N, Tanaka Y, Matsubara H.** 1983. Chimeramycins: new macrolide antibiotics produced by hybrid biosynthesis. J. Antibiot. **36:**927–930.